GCAGS JOURNAL
A Publication of the Gulf Coast Association of Geological Societies
www.gcags.org

High-Resolution Rock Strength and the Implications for Reservoir Geomechanics in the Cenomanian-Age Buda Formation, Dimmit County, Texas

Christopher K. Zahm[1], Robert G. Loucks[1], and Bruce G. Gates[2]

[1]*Bureau of Economic Geology, Jackson School of Geosciences, University of Texas at Austin, University Station, Box X, Austin, Texas 78713–8924, U.S.A.*

[2]*Ageron Energy, LLC, San Antonio, Texas 78729, U.S.A.*

ABSTRACT

The Buda Formation is a productive, naturally fractured reservoir unit in South Texas that has undergone a resurgence in development using horizontal wells and hydraulic stimulation to produce from low-porosity zones. A rich dataset that includes core, dipole sonic logs, and formation microresistivity (FMI) image logs within the Buda interval was collected for the McKnight 1305H in Dimmit County, Texas. Unconfined compressive strength (UCS) values are high in the Buda Formation in this well with a mean value of 89.5 MPa (~13,900 psi) compared to other stratigraphic formations in this well (e.g., Austin Chalk Group, Eagle Ford Group, and Del Rio Formation). However, the key issue within the Buda is that UCS values vary between the two predominant lithofacies—lime wackestone and argillaceous mudstones. Mean of all measured UCS values within the lime wackestone lithofacies is 93.9 MPa (~13,600 psi) with a standard deviation of 17.9 MPa (~2600 psi) compared to argillaceous mudstone that has a mean UCS of 86.0 MPa (~12,400 psi) with a standard deviation of 19.5 MPa (~2800 psi). There are also a few thin, limited bentonite beds that have UCS values of 10–30 MPa (~1500–4400 psi). Measured UCS in core shows a correlation between UCS, porosity, and other rock mechanics data. Observation of drilling-induced tensile fractures and borehole breakouts in FMI logs are used to determine a 052° azimuth (N52°E) of horizontal maximum stress (SHmax). These observations, combined with knowledge of the UCS of the Buda enable the construction of a stress polygon that is used to determine that the McKnight well lies within the strike-slip (SS) stress state regime where the SHmax is greater than the overburden stress (Sv), which in turn is greater than the minimum horizontal stress (Shmin). This is likely related to location of the McKnight well, which is drilled along an antiformal feature associated with the Chittim Anticline that formed during the Laramide Orogeny approximately 30 Ma.

INTRODUCTION

The resurgence of hydrocarbon exploration and development from tight carbonate reservoirs has created renewed interest in Late Cretaceous chalks including the Buda Formation. Modest success has been achieved in Buda production (Petzet, 1990; Darbonne, 2012; Davis et al., 2016) yet little is known about the source of permeability architecture in this tight matrix reservoir (Loucks et al., 2019, this volume). In many cases, permeability in the Buda is developed within natural fractures (Snyder and Craft, 1977; Stapp, 1977; Parker, 2000; Smirnov and Liner, 2018). Formations like the Buda exhibit variable rock strength lithofacies, which can cause heterogeneous natural fracture development (Corbett et al., 1987; Gross, 1993; Ferrill and Morris., 2008; Zahm et al., 2010). Furthermore, the Buda is targeted as a potential hydraulic fracture stimulation candidate and necessitates information regarding the rock strength variability within the formation. The combination of detailed core lithofacies, high-resolution core measurements of rock strength, and characterization of the current stress state, including the magnitude of the minimum horizontal principal stress state, make this study a valuable contribution to the understanding of the Buda Formation in a poorly characterized location of the Maverick Basin.

This study documents high-resolution unconfined compressive strength (UCS) measurements are measured on core and an estimate of the horizontal minimum stress state within the US Enercorp 1305H McKnight well is performed in the Buda Formation in Dimmit County, Texas (Fig. 1). The lithofacies, pore types, and reservoir quality of the cores are described in Loucks et al. (2019, this volume) and highlight that the well has two

Manuscript received April 8, 2019; revised manuscript received May 10, 2019; manuscript accepted June 21, 2019.

GCAGS Journal, v. 8 (2019), p. 268–280.
DOI: pending

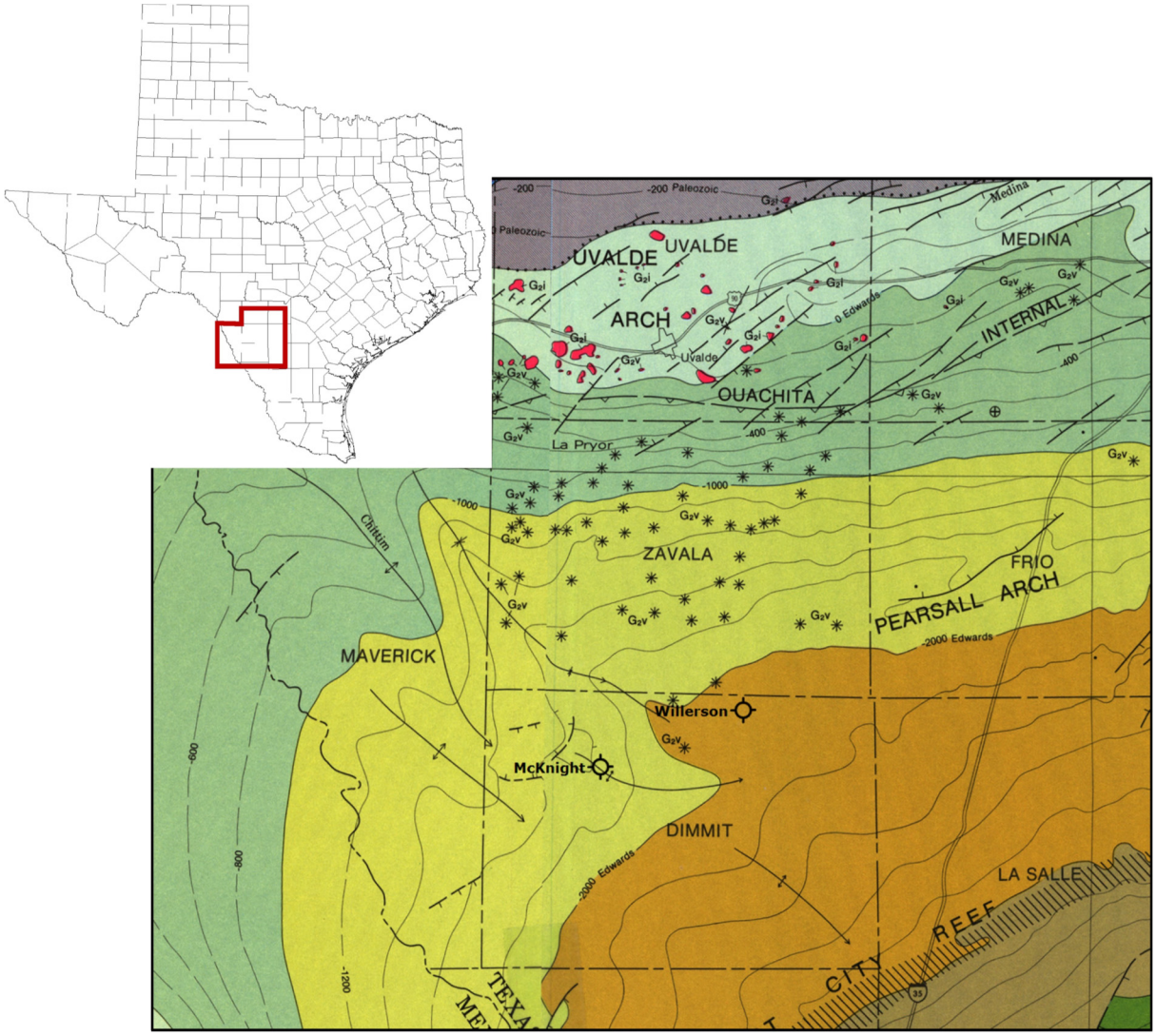

Figure 1. Location of the McKnight 1305H core superimposed on the Tectonic Map of Texas (Ewing, 1990). This map highlights that the McKnight well (top Buda, -1515 m [-4972 ft] subsea elevation) is located on a structural arch that extends from the Chittim Anticline to the northwest. These structures formed during Laramide Orogeny and antiformal structures are common to the southwest in northeastern Mexico.

main lithofacies (i.e., lime wackestone and argillaceous mudstone). Measurement of the high-resolution UCS values from core was accomplished in conjunction with a neutron porosity and dipole-sonic logs. A formation microresistivity image (FMI) log is used to determine the subsurface stress conditions, including magnitude and orientation of the maximum and minimum horizontal stresses. Objectives of this study are to: (1) measure UCS at a high-resolution scale; (2) compare measured values to lithofacies described in core; (3) analyze the log-measured petrophysical properties compared to the core rock properties; and (4) utilize characterized stress related features from the FMI log in combination with rock properties measured in core to assess the current-day stress state of the strata in the McKnight well.

GEOLOGIC BACKGROUND

The McKnight S 1305H (unique well identifier [UWI] = 4212736333000) well is located within the Maverick Basin which is the northwestern end of the Rio Grande Embayment of the Gulf of Coast Basin (Rose, 1984) and cores through the Cenomanian-age Buda Formation which is a fractured-chalk hydrocarbon producer. The western side of the Maverick has several notable regionally mapped structures including the Eagle Pass Anticline and Syncline, the Chittim Anticline, and Zavala Syncline (Rose, 1984; Ewing, 1987; Ewing, 2011). The Chittim Anticline is a Laramide-age (~80–40 Ma) antiformal structure described by Fowler (1956), but mapped in detail in the subsurface by Rose (1984) and imaged with seismic data and published in Scott (2004). The main portion of Chittim Anticline is contained within Maverick County, but the plunging southeastern nose continues as a minor structure in Dimmit County (Fig.1).

The northern Maverick Basin has undergone several significant tectonic events including the Pennsylvanian Ouachitan Orogeny, a failed rift event in the Late Triassic, Late Cretaceous volcanism, Late Cretaceous to Tertiary Laramide Orogeny, and finally Oligocene Gulf of Mexico marginal extension (Ewing, 2003, 2010; Treadgold et al., 2010) including extensional faulting associated with the Balcones Fault Zone (Collins and Hovorka, 1997; Ferrill et al., 2004, 2011; Ferrill and Morris, 2008). This latest extensional faulting is a result of gravitational sliding and extension related to the subsidence of the Gulf of Mexico Basin.

The current day stress regime of the Maverick Basin is considered normal faulting (NF) (Heidbach et al., 2016; Lund Snee

and Zoback, 2016) with a NNE–trending maximum horizontal stress (SHmax) direction in the western Maverick Basin, which is rotated to ENE azimuth on the eastern side of the basin. Local areas of the basin experience minor overpressure, but overall the basin generally has normal pore pressure (Ewing, 2011).

The Buda Formation is a fractured chalk reservoir deposited on the broad, Late Cretaceous drowned shelf and is stratigraphically between the underlying Del Rio Formation and overlying Eagle Ford Group. Loucks et al. (2019, this volume) describe two key lithofacies in the Buda—the lime wackestone and argillaceous mudstone. The lithofacies distinction is important for understanding and predicting fracture development in the subsurface.

METHODS

This study characterizes UCS every 10 cm (4 in) along the entire Buda interval using a micro-rebound hammer, which is a proven nondestructive technique (Verwaal and Mulder, 1993; Becerra and Matsukura, 2008; Zahm and Enderlin, 2010; Lee et al., 2014; Ritz et al., 2014; Brooks et al., 2016). For each recorded measurement, a minimum of 10 individual micro-rebound hammer strikes were made using an Equotip Piccolo device. Care was taken to measure on the thickest portion of the core, away from edges and pre-existing cracks. The highest and lowest strike values were dropped and the remaining eight or more individual strikes were averaged to a reported mean value. Values are reported in Leeb units and converted to UCS using the conversion equation and correction from Brooks et al. (2016).

Measured values for UCS were imported into Petra software, where the values measured on the core could be depth shifted. Minor depth shifts were made to ensure the UCS and core matched the wireline logs. The core depth shifts were applied to the UCS values, core characterized lithofacies descriptions.

After the core and logs were properly shifted, comparisons between wireline measured log values and the core-measured UCS were performed. UCS is a rock property related to the acoustic properties of the formation and comparisons were made to the wireline-log curves that are most correlative to UCS including neutron porosity (NPHI) and dipole sonic log measured dynamic Young's Modulus (YME_d) and dynamic Poisson's Ratio (PR_d). Cross plots of co-located core versus wireline measured values were developed.

Interpretation of the FMI log by Schlumberger noted the presence of drilling-induced tensile along with borehole breakouts. Orientation of the drilling-induced fractures and breakouts is used to determine the direction of the maximum and minimum horizontal stress (SHmax and Shmin, respectively). The overburden or vertical gradient (Sv) of 0.0238 MPa/m (1.05 psi/ft) is used to determine the overburden or vertical stress (Sv) within the Buda reservoir at depth. Pore pressure is constrained using mud weight data. We use stress gradient to generalize the results for application in a depth independent context. A coefficient of sliding friction (μ) of 0.7 is used for the Buda Formation because it has a high average UCS and is a low-porosity limestone. Using these observations, a stress polygon is developed using the techniques of Moos and Zoback (1990) and Zoback (2007).

Values of SHmax and Shmin are constrained by two lines that are superimposed on the stress polygon. The first is the borehole breakout line, which is determined by the UCS of the formation and sets the limit line for borehole breakout development. The second superimposed line is the drilling-induced fracture line, which marks the portion of the polygon where tensile fractures develop while drilling. The portion of the stress polygon that lies above these two lines then constrains the possible values of SHmax and Shmin (assumed equal to the formation closure stress).

RESULTS AND DISCUSSION

The primary purpose of measuring the UCS at high-resolution is to better understand the average properties of different lithofacies, especially the lime wackestone and argillaceous mudstone lithofacies. Within the Buda interval, 436 UCS measurements were collected (Fig. 2) and have a mean value of 89.5 MPa (~12,900 psi) with a standard deviation of 19.4 MPa (~2800 psi). The distribution of measured values ranges from 10 MPa (1450 psi) to 122 MPa (~17,700 psi), but is skewed toward the higher values with a mode value 107.4 MPa (~15,600 psi). Overall these values are higher than other zones of interest (e.g., Del Rio, Eagle Ford, and Austin Chalk) measured with the same techniques (Zahm and Enderlin, 2010; Brooks et al., 2016).

Assessment of the UCS values by facies was done by dividing the readings into two dominant lithofacies—lime wackestone and argillaceous mudstone—identified in the McKnight core (Loucks et al., 2019, this volume). Mean measured UCS values within the wackestone lithofacies is 93.9 MPa (~13,600 psi) with a standard deviation of 17.9 MPa (~2600 psi) compared to the mean UCS of 86.0 MPa (~12,400 psi) with a standard deviation of 19.5 MPa (~2800 psi) for the argillaceous mudstone lithofacies (Fig. 3). These distributions are weighted toward the higher UCS values and the modes are 107.4 MPa (~15,600 psi) and 96.6 MPa (~14,000 psi) for the lime wackestone lithofacies and the argillaceous mudstone lithofacies, respectively.

The average, mode, and standard deviation of the two lithofacies does not fully demonstrate the differences of the two lithofacies, nor does it allow for thinking about how to best correlate the properties to the overall stratigraphic framework. The UCS values must be plotted beside the core description to best understand the variability in rock strength and to visualize how the low UCS values define the mechanical stratigraphy of the Buda (Fig. 4). For this study the core description of Loucks et al. (2019, this volume) was digitized and depth shifted with the measured UCS along with an argillaceous lithofacies flag to provide the best view (Fig. 4, columns 2, 3, and 4). The log display now enables the view of the relationship between the lime wackestones (light blue) and the argillaceous mudstones (gray) and argillaceous beds (column 3). The UCS values are highly variable within the argillaceous mudstone facies compared to the lime wackestone facies which tend to have higher UCS and less variability. From this view, the packaging of common UCS units better informs on the mechanical stratigraphic framework of the Buda within the McKnight well.

Comparison of Measured UCS to Wireline Logs

The second objective of this study is to compare the measured values of UCS to wireline logs of similar resolution for improved correlation beyond the cored wells. Measured UCS are compared to NPHI and sonic log measured YME_d and PR_d at the same location (columns 4 and 5 in Figure 4). Overall, the general shape of the curves is consistent with the core facies description with the UCS being higher in lime wackestone facies and somewhat lower in the argillaceous mudstone. Variations in the NPHI and PR_d (inversely correlated to UCS), YME_d (positively correlated with UCS), and facies descriptions suggest that a mechanical stratigraphic framework is emerging from the data.

Porosity has been shown to have an effect on UCS (Chang et al., 2006; Dewhurst et al., 2010; Chen et al., 2015) and a correlation between the measured UCS and NPHI log within the McKnight well reveals a consistent but clouded correlation (Fig. 5). A tight cluster of data in the upper left of the cross plot illustrates that low-porosity rock usually correlates to higher UCS values. The lime wackestone is generally very low porosity, whereas the argillaceous mudstone is more variable. Loucks et al. (2019, this volume) document the effect of mudflows on UCS with the in-place facies being stronger than resedimented mud-

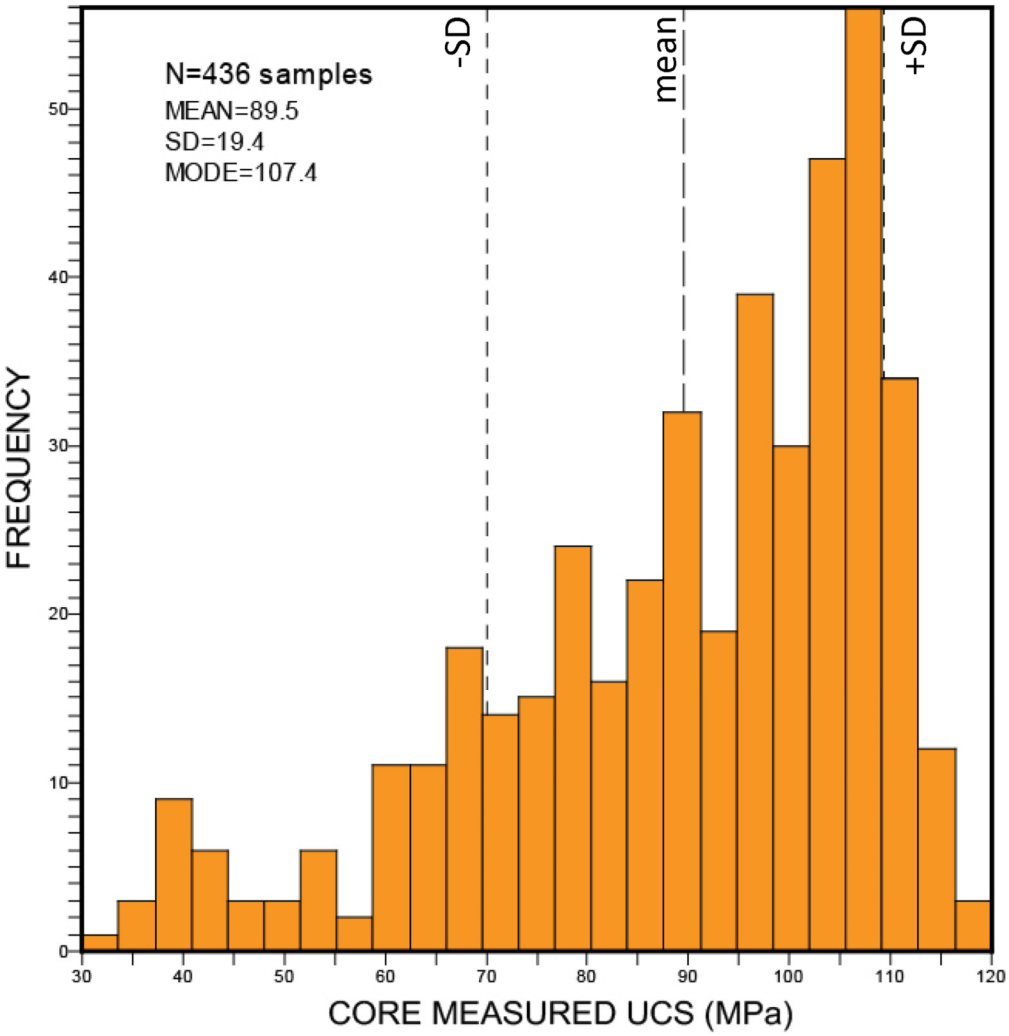

Figure 2. Histograms of core measured UCS for the Buda Formation in the McKnight core. The mean value is 89.5 MPa (~13,900 psi) with a mode of 107.4 MPa (~15,600 psi). Dashed lines mark the mean and standard deviation of the sampled values. 10 MPa = ~1450 psi.

flows of the same facies. High-resolution sampling of UCS with the micro-rebound hammer is unique as the sample size is less than 1 cm (0.4 in), which is on the scale of the thin-bedded argillaceous mudstones. Resolution of the NPHI log is significantly coarser at around 0.6–0.9 m (2–3 ft). The variability in scale of resolution may be one of the causes of the data scatter in the cross plot as the well log NPHI scale is averaging significantly greater thickness of rock compared to the UCS measurements.

Many of the poroelastic equations for prediction of stress and rock strength in the subsurface use Young's Modulus and Poisson's Ratio. A cross plot of the values for these two parameters in the McKnight well (Fig. 6) shows that PR_d is consistent with values of tight limestone or chalk ranging from 0.26–0.32 (Chang et al., 2006). However, the YME_d values are high compared to published values, which are typically 10–60 GPa ($1.45x10^6$–$8.70x10^6$ psi) (Friedman and Wiltschko, 1992; Rijken and Cooke, 2001). Data on the cross plot was colored by variable UCS values measured in core (Fig. 6). The highest values of UCS correspond to the highest values of YME_d, whereas the lower UCS values are more variable, but tend to plot in the lower values of YME_d and PR_d. This is highlighted by the histograms included on the cross plot axes in Figure 6.

A different approach is used to understand the relationship between UCS, PR_d, YME_d, and lithofacies described in the McKnight core. Here, we plot core measured UCS against YME_d/PR_d (Fig. 7), which is a proxy calculation for brittleness of the rock (Rickman et al., 2008). The points on the cross plot are colored by lithofacies and highlight that the low porosity, lime wackestone lithofacies has the highest UCS values and brittleness (YME_d/PR_d). The argillaceous lithofacies is more variable, similar to Figure 4. Resolution of the YME_d and PR_d logs contributes to the cause of scatter in the data.

Overall, the wireline log and core-measured UCS values are correlative and consistent with previous work on UCS measurements in tight reservoirs (Sone and Zoback, 2013; Amendt et al., 2013; Becerra et al., 2018). One observation that stands out is that the Buda has higher YME_d and UCS than other similar stratigraphic sections (e.g., Austin Chalk). As a result, the Buda is more likely to fracture during deformation, but only after a significant amount of differential stress is applied to the formation.

RESERVOIR GEOMECHANICS APPLICATION

The third objective of this study is to use the results of the UCS measured properties to characterize the reservoir stress state including the magnitude of the formation closure stress (Shmin), and the magnitude and orientation of SHmax. Existing data from the McKnight well is a relatively complete dataset that has core data and dipole sonic log, density, and FMI logs through the same intervals enabling the calculation of stress magnitudes and orientations in the well. The FMI from the McKnight well through the Buda interval (1734–1743 m [5707–5720 ft] measured depth [MD]) (Fig. 8) was acquired and interpreted by Schlumberger for U.S. Enercorp. The FMI log shows drilling-

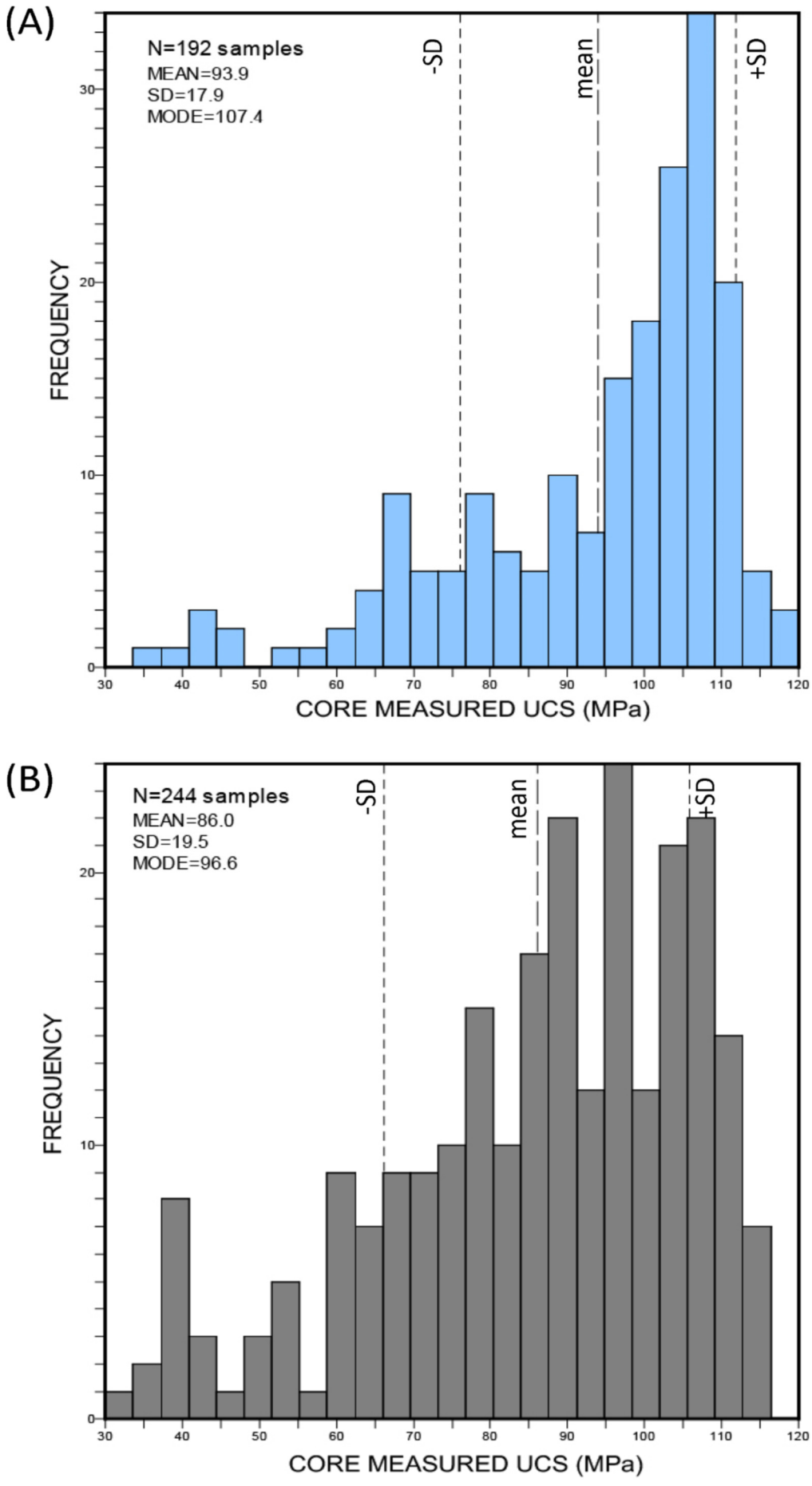

Figure 3. Histograms of core measured UCS for the Buda Formation in the McKnight core for the two main facies of Loucks et al. (2019, this volume). (A) Histogram of UCS values for wackestone limestone facies (mean = 93.9 MPa [~13,600 psi], mode=107.4 MPa [~15,600 psi]). (B) Histogram of UCS values for argillaceous facies (mean = 86.0 MPa [~12,400 psi], mode = 96.6 MPa [~14,000 psi]). 10 MPa = ~1450 psi.

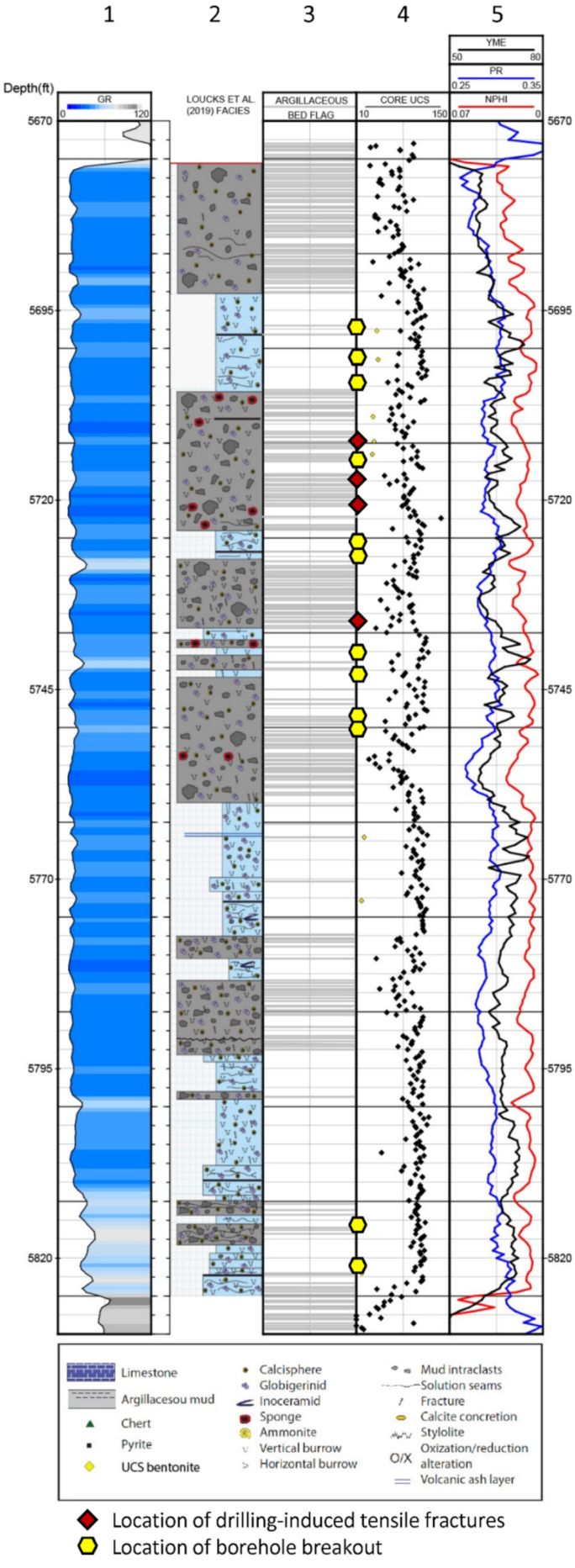

Figure 4. Well log for the McKnight core through the Buda Formation. Column 1 is the gamma ray (GR) shaded to highlight zones of increasing GR. Column 2 is described facies and fabric observed in core and presented in Loucks et al. (2019, this volume). Column 3 is an argillaceous flag where each bed is marked supporting the core description and influencing the variation of UCS within each facies. Column 4 is the core measured UCS (MPa) at 436 locations within core. Between columns 3 and 4 are symbols that mark the interval with observed drilling-induced tensile fractures (red diamond) and borehole breakouts (yellow hexagon) from the FMI log through the McKnight well. Column 5 is the dynamic Young's Modulus (labeled as YME), dynamic Poisson's Ratio (labeled as PR) and neutron porosity (NPHI) from the wireline log in the McKnight well.

induced tensile fractures as well as borehole breakouts within the Buda interval. Comparison of the core to the FMI reveals that the interpreted low-angle fractures are actually disturbed bedding from frequent mud flows or plumes within the Buda (see Loucks et al., 2019, this volume). Overall, natural, conductive (open) fractures are rare within the Buda interval.

Drilling-induced tensile fractures and breakouts are interpreted throughout the Buda interval (Fig. 8). Measured borehole breakouts and drilling-induced fractures are recognized in the McKnight well (Fig. 9). Based on these measured features, SHmax is interpreted to have an azimuthal orientation of 052° (N52°E) and Shmin is oriented along an azimuth of 322° (N38° W) using techniques of Zoback et al. (1985). This orientation of SHmax is consistent with observations of Lund Snee and Zoback (2016) for the Karnes County area (N45°E). However, there is a rotation from a near NNE (N10°E) oriented SHmax in western Maverick County to the McKnight well in Dimmit County. This apparent rotation likely reflects the underlying basement structure which changes from a NNW–oriented Triassic rift system (Rose, 1984) on western side of the Maverick Basin to the ENE–oriented Balcones Fault system to the north. It is unclear if the rotation in SHmax direction is indicative of significant variability in the stress regime in the McKnight well.

Stress polygons are a useful technique to constrain the stress magnitudes in a well bore. Using the methods of Moos and Zoback (1990) and Zoback (2007), a stress polygon is constructed for the McKnight well (Fig. 10). Two lines are added to the stress polygon—the induced-fracture and borehole breakouts present line. In the case of the McKnight well, both features are observed. The borehole breakout line is a function of the UCS of the rock and assumed to be 90 MPa (~13,050 psi) based on measured UCS in core. Based on the stress polygon, SHmax > Sv > Shmin within the McKnight well and, as such, the current stress state is within the strike-slip (SS) fault regime. This is unusual compared to other wells in the Maverick Basin, which are typically within the normal fault (NF) regime (Lund Snee and Zoback, 2018). This is an important conclusion as it highlights variability in the stress state along a minor structural fold (parallel to the Chittim Anticline) and probably reflects a latent Laramide orogenic (compressional) stress state.

In the case of the McKnight well, the determination that the reservoir is in a SS regime is largely dictated by the presence of borehole breakouts and the UCS measured in core. In order to ensure that the proper UCS value was used, a sensitivity test was conducted. The same stress polygon is used, but the UCS values are changed to the lower standard deviation of the argillaceous mudstones (66 MPa [~9570 psi]) and a new breakout-presence line is plotted (Fig. 11). For a high-side case, we also plot a breakout-present line for the high-side standard deviation of the lime wackestone (Fig. 11). In either case, we are within the SS regime of the stress polygon.

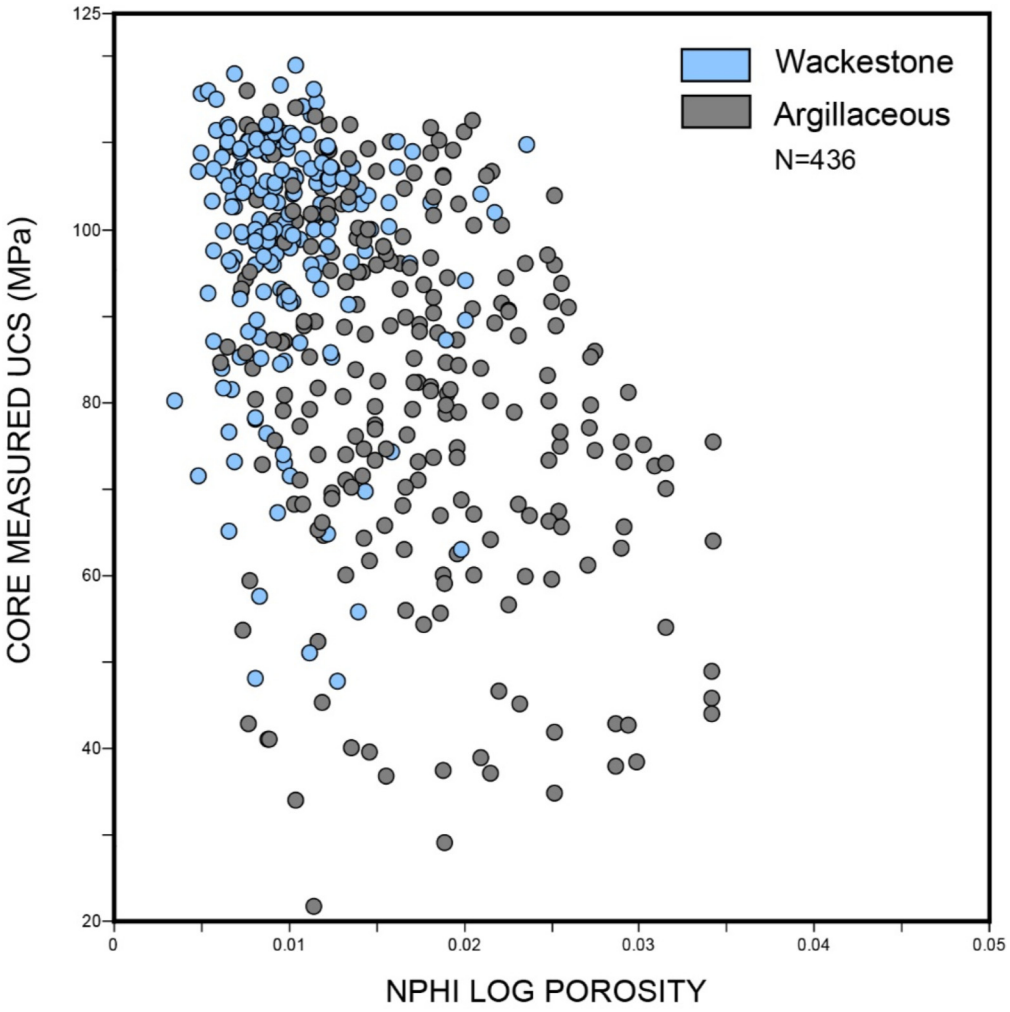

Figure 5. Cross plot of measured UCS values against log neutron porosity (NPHI) separated by two dominant lithofacies within the Buda Formation. The tight lime wackestone has low porosity and high UCS values. The argillaceous mudstone lithofacies has more heterogeneous UCS values but also has higher porosity. NPHI is in limestone matrix units.

For many reservoirs, Shmin is considered to be equivalent to the formation closure stress. Using the endmembers of UCS as a guide, the range of values of Shmin (formation closure stress) can vary from 29 MPa (~4200 psi) to 36 MPa (~5100 psi). Formation closure stress gradients are calculated to be from 0.0167 MPa/m (0.74 psi/ft) to 0.0185 MPa/m (0.82 psi/ft). It is important to know the relative ratio between the magnitudes of Shmin and SHmax to understand if the reservoir is highly anisotropic, as this can lead to significant difference in hydraulic fracture propagation or cause areas of critically-stressed faults and fractures within the reservoir interval (e.g., Hennings et al., 2012). It is important to know the relative ratio between the magnitudes of Shmin and SHmax to understand if the reservoir is highly anisotropic. In the case of the McKnight well, the SHmax to Shmin ratio varies between 1.6 to 2.5.

The lithofacies described within the Buda, specifically the argillaceous mudstone facies, may have an additional complication that creates the need for higher differential stress to be imposed on the formation in order to hydraulically stimulate the formation. Sone and Zoback (2014) highlighted the propensity of clay-rich rocks to deform by creep, effectively dissipating differential stress required to propagate a hydraulic fracture within the clay-rich portions of the formation. Under similar differential stress load, the higher UCS rocks will propagate fractures at a lower differential stress. This has important implications for the successful development of the mixed lithofacies of the Buda Formation.

The observation of the SS stress state seems unique to a basin that has largely been subsiding because of compaction for the past 15 Ma. However, the McKnight well is located on one of most northeastern antiformal features, the Chittim Anticline, along the Laramide Orogenic front (Ewing, 1990; Ferrill et al., 2014). Further investigation of the stress state, including earthquake data, microseismic response, or leak off tests would help to substantiate this finding, but is beyond the scope of this study.

CONCLUSIONS

A rich dataset that includes core data and dipole sonic, density, and FMI logs within the Buda interval was collected for the McKnight 1305H in Dimmit County, Texas. Measured UCS in core shows a correlation between UCS, porosity, and other rock mechanics data. Additional knowledge is gained when the rock properties are investigated using lithofacies described in the core. Overall, the Buda has high UCS values compared to comparable intervals (e.g., Austin Chalk). Observation of drilling-induced tensile fractures and borehole breakouts in FMI logs combined with knowledge of the UCS of the Buda enable the construction of a stress polygon and determine that the McKnight well lies within the SS regime in its current day stresses where the SHmax is greater than the overburden stress. This is likely related to location of the McKnight well, which is drilled along an antiformal feature associated with the Chittim Anticline that formed during the Laramide Orogeny approximately 30 Ma.

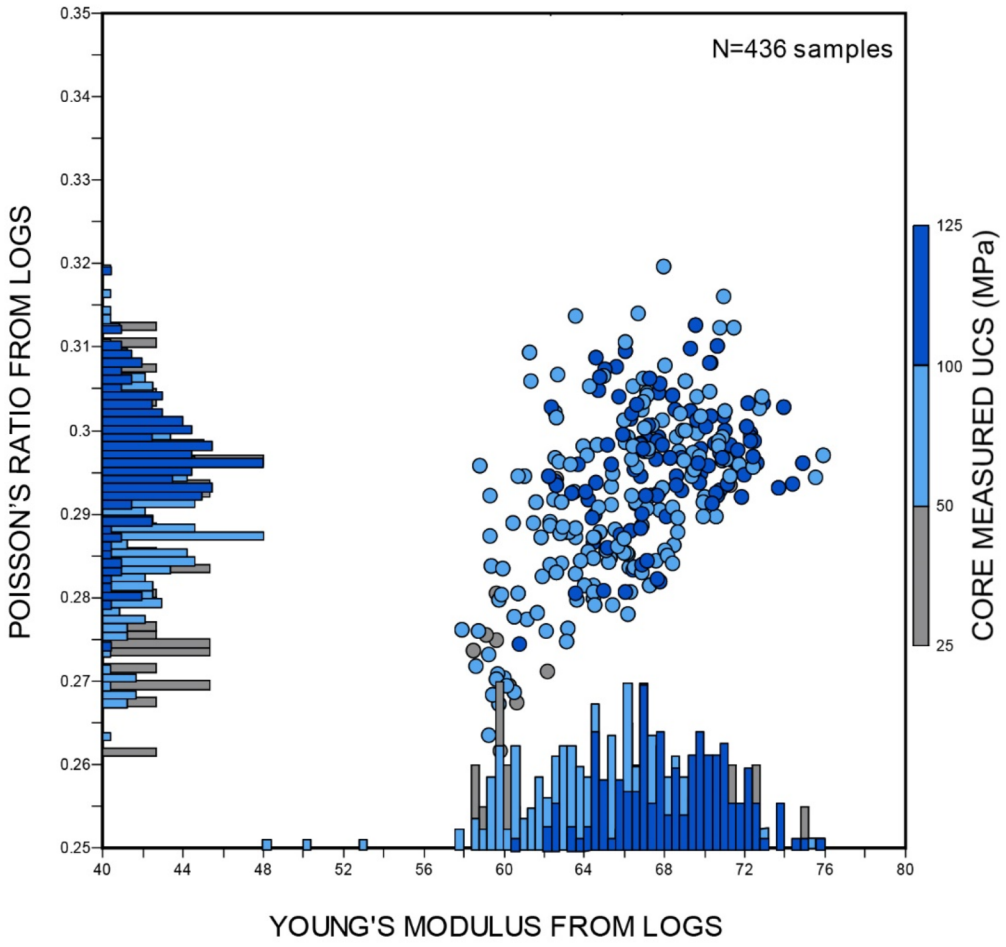

Figure 6. Cross plot of log measured dynamic Poisson's Ratio (PR_d) and dynamic Young's Modulus (YME_d) colored by the measured UCS values in core at similar depths. Histograms added to highlight the distribution of the data for each axis. In general, the highest UCS values have higher YME_d and somewhat lower PR_d whereas the lower UCS values correlate to lower YME_d and higher PR_d values.

ACKNOWLEDGMENTS

We want to recognize the Carbonate Reservoir Characterization Research Laboratory (RCRL) at the Bureau of Economic Geology and associated sponsors for support of this investigation. Thank you to Ageron Energy, LLC and Jeanne Flowers for her help to coordinate data and information transfer. We appreciate the reviews of the manuscript by Donald Brooks, Helge Alsleben, and Jens Lund Snee. Publication authorized by the Director, Bureau of Economic Geology, Jackson School of Geosciences, University of Texas at Austin.

REFERENCES CITED

Amendt, D., S. Busetti, and Q. Wenning, 2013, Mechanical characterization in unconventional reservoirs: A facies-based methodology: Petrophysics, v. 54, p. 457–464.

Aoki, H., and Y. Matsukura, 2008, Estimating the unconfined compressive strength of intact rocks from Equotip hardness: Bulletin of Engineering Geology and the Environment, v. 67, p. 23–29.

Becerra, D., H. Galvis, and R. Slatt, 2018, Characterizing the two principal rock types comprising the Woodford Shale resource play: Application to shale geomechanics. Interpretation, v. 6, p. SC67–SC84.

Brooks, D., X. Janson, and C. K. Zahm, 2016, The effect of sample volume on micro-rebound hammer UCS measurements in Gulf Coast Cretaceous carbonate cores: Gulf Coast Association of Geological Societies Journal, v. 5, p. 189–202, <https://www.gcags.org/Journal/2016.GCAGS.Journal/2016.GCAGS.Journal.v5.11.p189-202.Brooks.et.al.pdf>.

Chang, C., M. D. Zoback, and A. Khaksar, 2006, Empirical relations between rock strength and physical properties in sedimentary rocks: Journal of Petroleum Science and Engineering, v. 51, p. 223–237.

Chen, X., D. R. Schmitt, J. A. Kessler, J. Evans, and R. Kofman, 2015, Empirical relations between ultrasonic P–wave velocity, porosity and uniaxial compressive strength: Canadian Society of Exploration Geophysicists Recorder, v. 40, no. 5, p. 24–29.

Collins, E. W., and S. D. Hovorka, 1997, Structure map of the San Antonio segment of the Edwards aquifer and Balcones Fault Zone, south-central Texas: Structural framework of a major limestone aquifer: Kinney, Uvalde, Medina, Bexar, Comal, and Hays counties: Bureau of Economic Geology Miscellaneous Map 38, Austin, Texas, scale 1:250,000, 2 sheets.

Corbett, K., M. Friedman, and J. Spang, 1987, Fracture development and mechanical stratigraphy of Austin Chalk, Texas: American Association of Petroleum Geologists Bulletin, v. 71, p. 17–28.

Davis, G., G. Wilcox, M. Amone, S. Bruington, 2016, Rejuvenating the Buda Limestone reservoir in Texas by using crude oil and nitrogen injection in underbalanced regime: case history: Society of Petroleum Engineers Paper SPE–179115–MS, Richardson, Texas, 23 p.

Darbonne, N., 2012, Buda beneath: Oil and Gas Investor, <https://www.hartenergy.com/exclusives/buda-beneath-12375>.

Dewhurst, D. N., J. Sarout, C. Delle Piane, A. F. Siggins, M. D. Raven, and U. Kuila, 2010, Prediction of shale mechanical properties from global and local empirical correlations: Society of Exploration Geophysicists Technical Program Expanded Abstracts 2010, p. 2595–2599.

Ewing, T. E., 1987, The Frio River Line in South Texas—Transition from Cordilleran to northern Gulf tectonic regimes: Gulf Coast

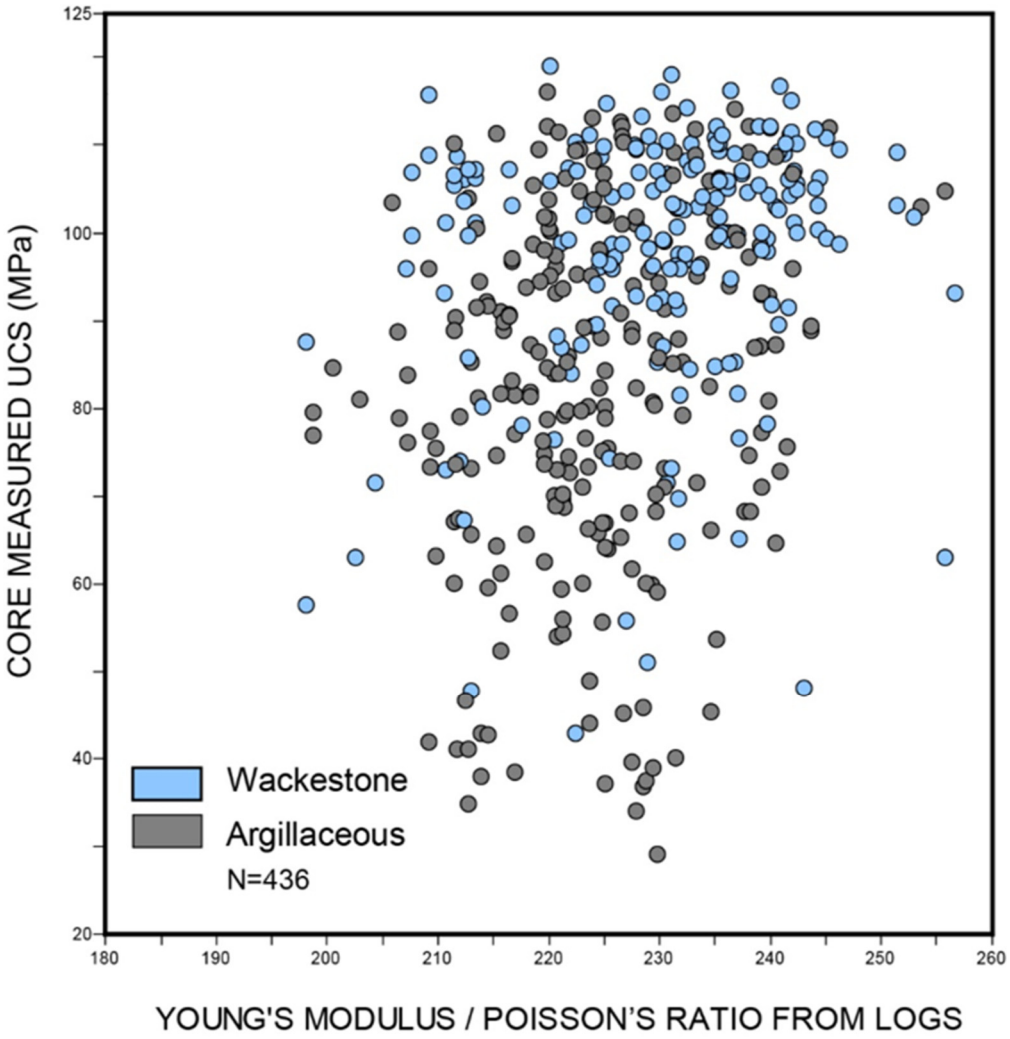

Figure 7. Cross plot of core measured UCS versus YME_d/PR_d which is often used as a proxy for brittleness (Rickman et al., 2008). As with previous plots, the wackestone lithofacies generally clusters in the higher UCS and brittle regions off the plot compared to the argillaceous mudstone lithofacies that has a broader range of measurements.

Association of Geological Societies Transactions, v. 37, p. 87–94.

Ewing, T. E., 1990, Tectonic map of Texas: Bureau of Economic Geology, Austin, Texas, scale 1:750,000, 4 sheets.

Ewing, T. E., 2003, Review of the Tectonic History of the Lower Rio Grande border region, South Texas and Mexico, and implications for hydrocarbon exploration: Society of Independent Professional Earth Scientists Newsletter, v. 40, p. 16–21.

Ewing, T. E., 2010, Pre-Pearsall geology and exploration plays in South Texas: Gulf Coast Association of Geological Societies Transactions, v. 60, p. 241–260.

Ewing, T. E., 2011, Tectonic domains in the Rio Grande / Rio Bravo border region, Texas and Mexico: Laramide structures suggest earlier history: Gulf Coast Association of Geological Societies Transactions, v. 61, p. 141–155.

Ferrill, D. A., D. W. Sims, D. J. Waiting, A. P. Morris, N. Franklin, and A. L. Schultz, 2004, Structural framework of the Edwards aquifer recharge zone in south-central Texas: Geological Society of America Bulletin, v. 116, p. 407–418.

Ferrill, D. A., and A. P. Morris, 2008, Fault zone deformation controlled by carbonate mechanical stratigraphy, Balcones Fault System, Texas: American Association of Petroleum Geologists Bulletin, v. 92, p. 359–380.

Ferrill, D. A., A. P. Morris, R. N. McGinnis, K. J. Smart, and W. C. Ward, 2011, Fault zone deformation and displacement partitioning in mechanically layered carbonates: The Hidden Valley Fault, Central Texas: American Association of Petroleum Geologists Bulletin, v. 95, p. 1383–1397.

Ferrill, D. A., R. N. McGinnis, A. P. Morris, K. J. Smart, Z. T. Sickmann, M., Bentz, D. Lehrmann, and M. A. Evans, 2014, Control of mechanical stratigraphy on bed-restricted jointing and normal faulting: Eagle Ford Formation, south-central Texas: American Association of Petroleum Geologists Bulletin, v. 98, p. 2477–2506.

Friedman, M. and D. V. Wiltschko, 1992. An approach to exploration for naturally fractured reservoirs, with examples from the Austin Chalk, *in* J. W. Schmoker, E. B. Coalson, and C. A. Brown, eds., Geological studies relevant to horizontal drilling: Examples from western North America: Rocky Mountain Association of Geologists, Denver, Colorado, p. 143–153.

Fowler, P., 1956, Faults and folds of south-central Texas: Gulf Coast Association of Geological Societies Transaction, v. 6, p. 37–42.

Gross, M. R., 1993, The origin and spacing of cross joints: Examples from the Monterey Formation, Santa Barbara coastline, California: Journal of Structural Geology, v. 15, p. 737–751.

Heidbach, O., M. Rajabi, K. Reiter, M. Ziegler, 2016, World stress map 2016: GFZ Data Services, Potsdam, Germany, <https://doi.org/10.5880/WSM.2016.002>.

Lee, J. S., L. Smallwood, and E. Morgan, 2014, New application of rebound hardness numbers to generate logging of unconfined compressive strength in laminated shale formations: Proceedings of the 48th U.S. Rock Mechanics/Geomechanics Symposium Paper 14–6972, Minneapolis, Minnesota, 1–4 June, 7 p.

Loucks, R. G., B. G. Gates, and C. K. Zahm, 2019, Depositional systems, lithofacies, nanopore to micropore matrix network, and

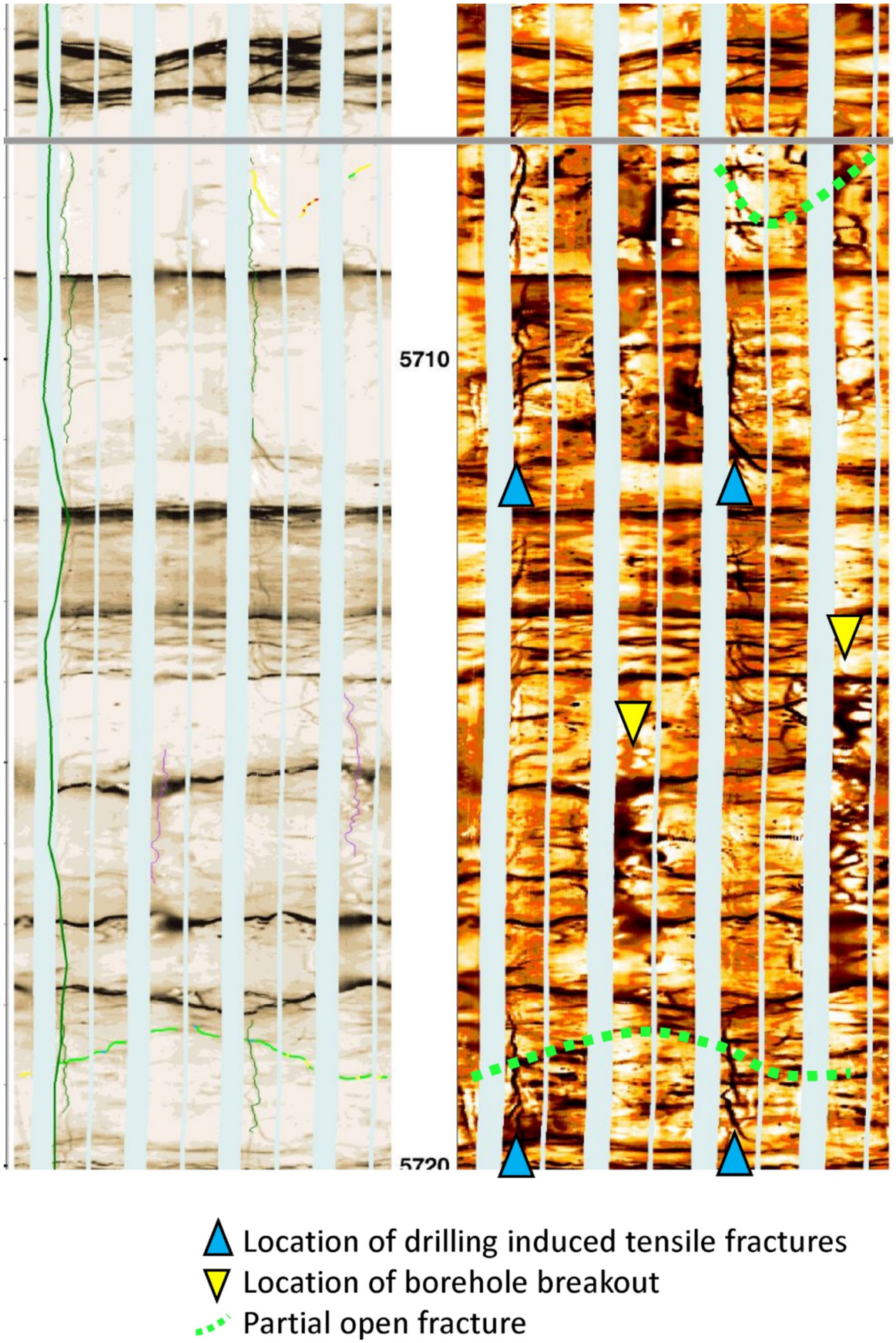

Figure 8. FMI from the McKnight well through the Buda interval highlighting drilling-induced tensile fractures, borehole breakouts, and partially open fractures (interpreted). The log was acquired and interpreted by Schlumberger for U.S. Enercorp. Comparison of the core to the FMI reveals that the interpreted low-angle fractures are actually disturbed bedding from frequent mud flows within the Buda (see Loucks et al., 2019, this volume).

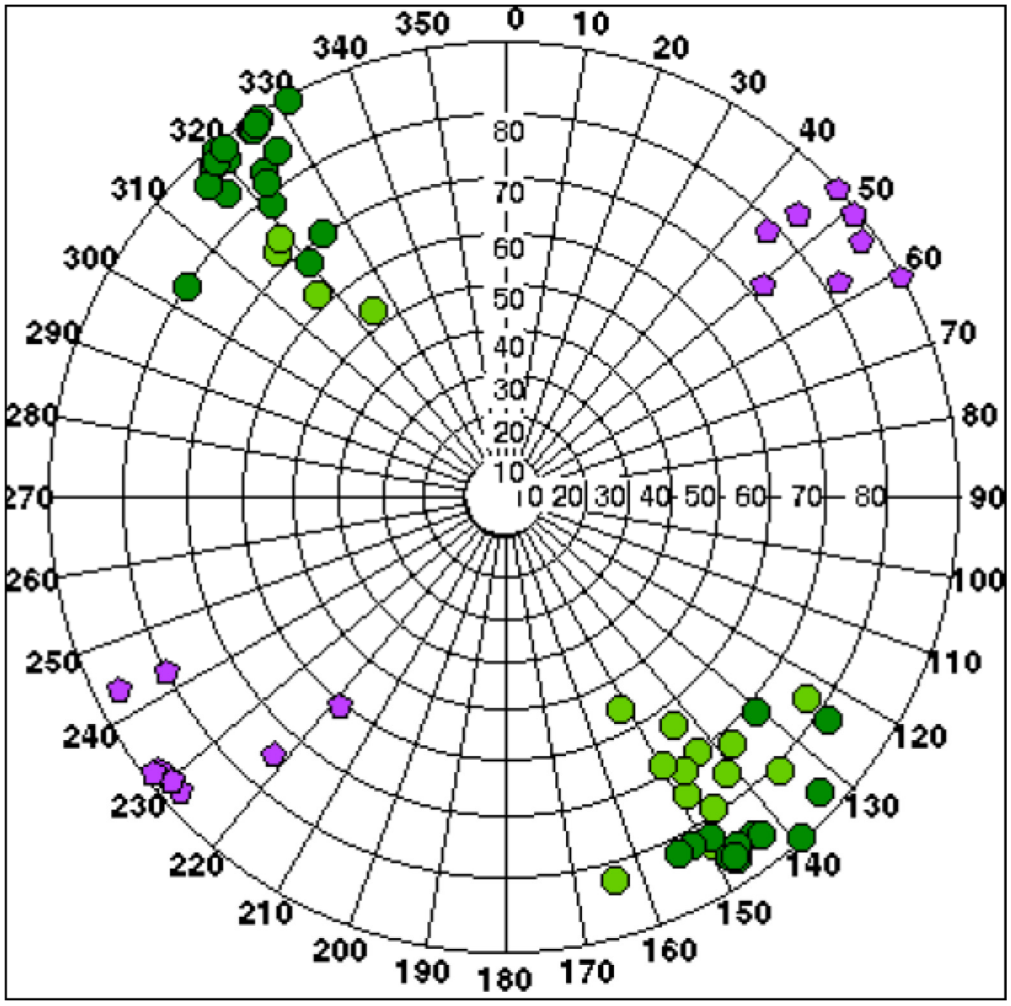

Figure 9. Upper hemisphere Wulff projection stereonet of measured borehole breakouts (purple hexagons) and drilling-induced fractures (dark green and light green circles) in the McKnight well. Based on these observations, SHmax is oriented on the azimuth 052° (N52°E) and Shmin is oriented 322° (N38°W). Both drilling-induced fractures and borehole breakouts can be observed in the Buda zones (see Figures 3 and 8).

reservoir quality of the Upper Cretaceous (Cenomanian) Buda Limestone in Dimmit County, southwestern Texas: Gulf Coast Association of Geological Societies Journal, v. 8, p. 281–300, <https://www.gcags.org/Journal/2019.GCAGS.Journal/2019.GCAGS.Journal.v8.15.p281-300.Loucks.et.al.pdf>.

Lund Snee, J. E., and M. D. Zoback, 2016, State of stress in Texas: Implications for induced seismicity: Geophysical Research Letters, v. 43, p. 10208–10214, <https://doi.org/10.1002/2016GL070974>.

Lund Snee, J.–E., and M. D. Zoback, 2018, State of stress in the Permian Basin, Texas and New Mexico: Implications for induced seismicity: The Leading Edge, v. 32, p. 127–134, <https://dx.doi/10.1190/tle37020127.1>.

Parker, R. M., 2000, The Lower Cretaceous Buda Limestone Formation in Gonzales County, Texas, and its potential as a fractured carbonate hydrocarbon reservoir: M.S. Thesis, Texas A&M University at Kingsville, 352 p.

Petzet, G. A., 1990, Buda strikes may boost South Texas action: Oil and Gas Journal, v. 88, no. 20, p. 25.

Rickman, R., M. J. Mullen, J. E. Petre, W. V. Grieser, and D. Kundert, 2008, A practical use of shale petrophysics for stimulation design optimization: All shale plays are not clones of the Barnett Shale: Society of Petroleum Engineers SPE–115258–MS, Richardson, Texas, 11 p.

Rijken, P. and M. L. Cooke, 2001, Role of shale thickness on vertical connectivity of fractures: Application of crack-bridging theory to the Austin Chalk, Texas: Tectonophysics, v. 337, p. 117–133.

Ritz, E., M. M. Honarpour, J. Dvorkin, and W. F. Dula, 2014, Core hardness testing and data integration for unconventionals: Society of Petroleum Engineers Paper SPE–2014–1916004–MS, Richardson, Texas, 12 p.

Rose, P. R., 1984, Oil and gas occurrence in Lower Cretaceous rocks, Maverick Basin area, southwest Texas, *in* C. I. Smith, ed., Stratigraphy and structure of the Maverick Basin and Devils River Trend, Lower Cretaceous, southwest Texas: A field guide and related papers: South Texas Geological Society, San Antonio, p. 80–93.

Scott, R. W., 2004, The Maverick Basin: New technology—New success: Gulf Coast Association of Geological Societies Transactions, v. 54, p. 603–620.

Smirnov, A., and C. L. Liner, 2018, Interpretation and fracture characterization of Upper Cretaceous Buda Limestone Formation using post-stack 3D seismic data in Zavala County, Texas: American Association of Petroleum Geologists Search and Discovery Article 11108, Tulsa, Oklahoma, 24 p., <http://www.searchanddiscovery.com/pdfz/documents/2018/11108smirnov/ndx_smirnov.pdf.html>.

Snyder, R. H., and M. Craft, 1977, Evaluation of Austin and Buda Formations from core and fracture analysis: Gulf Coast Association of Geological Societies Transactions, v. 27, p. 376–385.

Sone, H. and M. D. Zoback, 2013, Mechanical properties of shale-gas reservoir rocks—Part 2: Ductile creep, brittle strength, and their relation to the elastic modulus: Geophysics, v. 78, p. D393–D402.

Stapp, W. L., 1977, The geology of the fractured Austin and Buda formations in the subsurface of South Texas: Gulf Coast Association of Geological Societies Transactions, v. 27, p. 208–229.

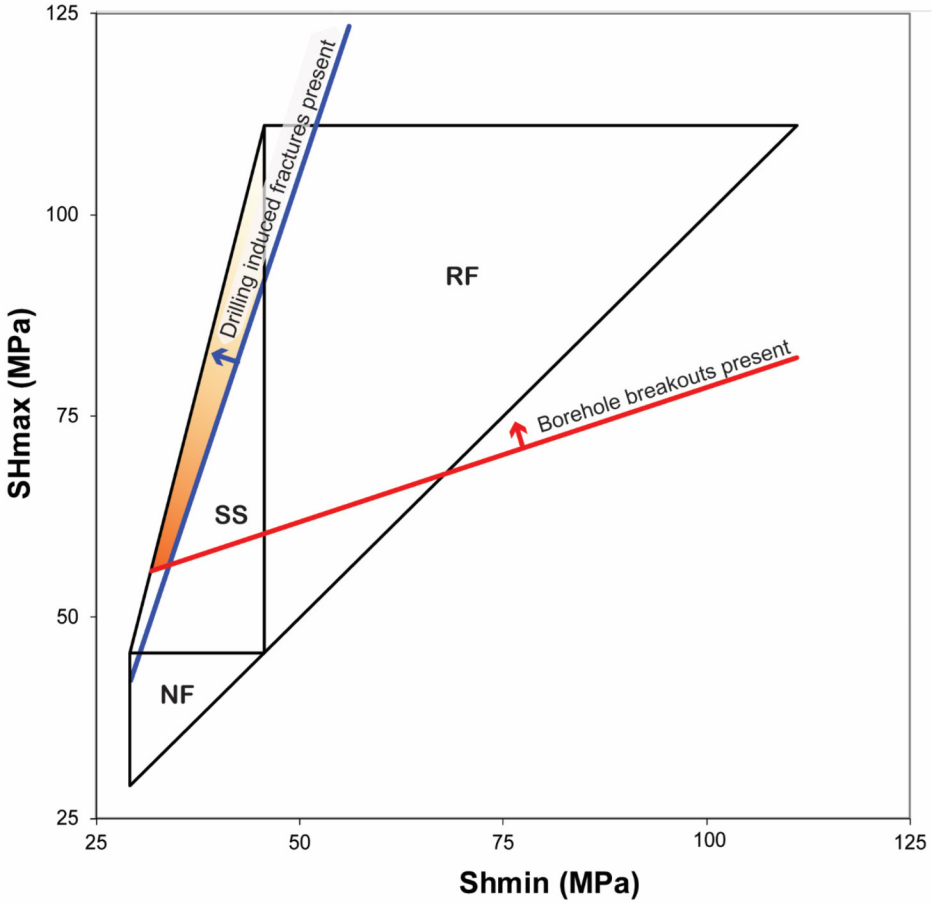

Figure 10. Stress polygon constructed from McKnight well data using the methods of Zoback et al. (1985) and Moos and Zoback (1990). For the McKnight well, both drilling-induced fractures and borehole breakouts were measured with the FMI tool. An assumed overburden gradient of 0.0238 MPa (1.05 psi/ft) was used to approximate Sv at 6615 psi (46 MPa) 46 MPa (~6615 psi) at a depth 1729.7 m (5675 ft) below surface. At that depth, a maximum present-day in-situ pore fluid pressure of 22.8 MPa (3305 psi) was calculated using mud weight data. The borehole breakout line is a function of the UCS of the rock and assumed to be 90 MPa (13,050 psi) based on average measured UCS in core and a coefficient of sliding friction of 0.7. Tensile strength of the rock determines the location of the induced fracture line. Based on the stress polygon, SHmax > Sv > Shmin within the McKnight well and is within the SS regime. Sensitivity analysis, however, does show that at lower pore pressures, weaker rocks (UCS less than 80 MPa [~11,600 psi]) would be within a SS or NF regime.

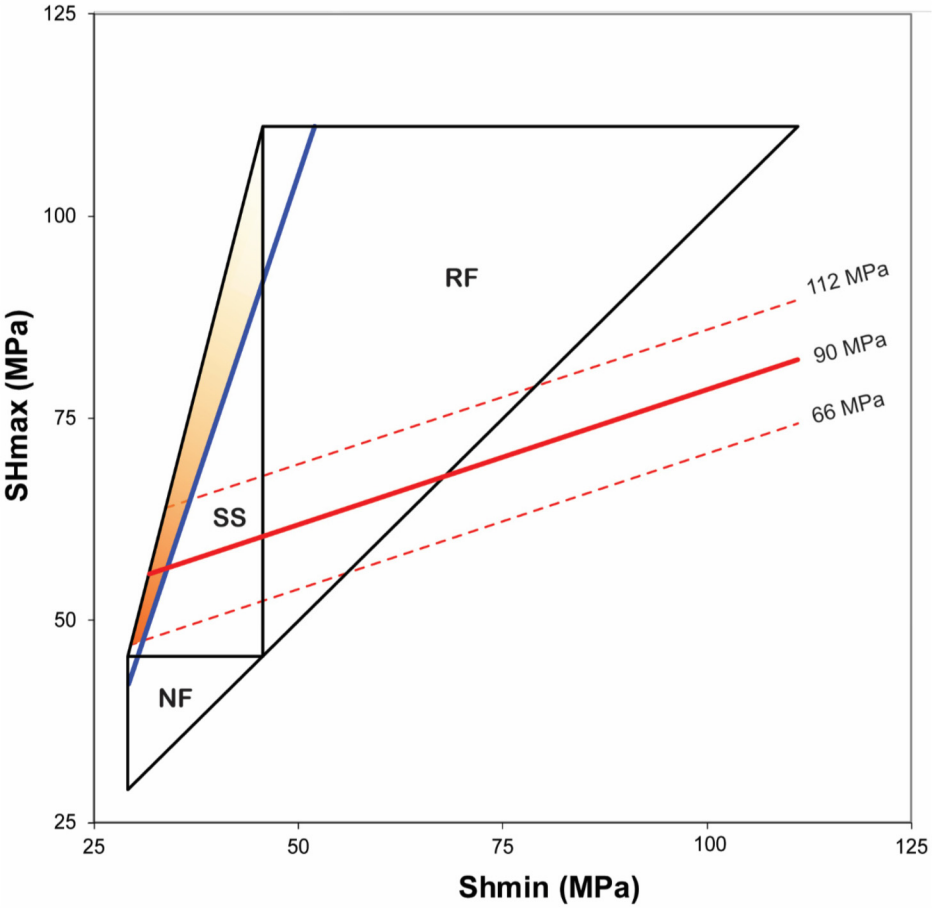

Figure 11. Based on the UCS values measured in the Buda core and presented in Figure 4, a potential range of 66 MPa (~9600 psi) from the lower standard deviation of argillaceous facies to 112 MPa (~16,200 psi) from higher standard deviation of wackestone lithofacies is possible for the Buda in the McKnight well. The range of values of Shmin (formation closure stress) is 29 MPa (~4200 psi) to 36 MPa (~5100 psi). Formation closure stress gradients range from 0.0167 MPa/m (0.74 psi/ft) to 0.0185 MPa/m (0.82 psi/ft). The SHmax/Shmin ratio ranges between 1.6 to 2.5.

Treadgold, G., B. McLain, S. Sinclair, and D. Nicklin, 2010, Eagle Ford Shale prospecting with 3D seismic data within a tectonic and depositional system framework: Bulletin of the South Texas Geological Society, v. 51, no. 1, p. 19–28.

Verwaal, W., and A. Mulder, 1993, Estimating rock strength with the Equotip hardness tester: International Journal of Rock Mechanics, Mining Science and Geomechanics Abstracts, v. 30, p. 659–662.

Zahm, C. K., and M. Enderlin, 2010, Characterization of rock strength in Cretaceous strata along the Stuart City Trend, Texas: Gulf Coast Association of Geological Societies Transactions, v. 60, p. 693–702.

Zahm, C. K., L. C. Zahm, and J. A. Bellian, 2010, Integrated fracture prediction using sequence stratigraphy within a carbonate fault damage zone, Texas, USA: Journal of Structural Geology, v. 32, p. 1363–1374, <https://doi.org/10.1016/j.jsg.2009.05.012>.

Zoback, M. D., D, Moos, L. Mastin, and R. N. Anderson, 1985, Well bore breakouts and in situ stress: Journal of Geophysical Research: Solid Earth, v. 90, p. 5523–5530, <https://doi.org/10.1029/JB090iB07p05523>.

Zoback, M. D., 2007, Reservoir geomechanics: Cambridge University Press, U.K., 449 p., <https://doi.org/10.1017/CBO9780511586477>.